AIP | Applied Physics Letters

Fabrication of uniform Ge-nanocrystals embedded in amorphous SiO2 films using Ge-ion implantation and neutron irradiation methods

Q. Chen, T. Lu, M. Xu, C. Meng, Y. Hu et al.

Citation: Appl. Phys. Lett. **98**, 073103 (2011); doi: 10.1063/1.3553770
View online: http://dx.doi.org/10.1063/1.3553770
View Table of Contents: http://apl.aip.org/resource/1/APPLAB/v98/i7
Published by the AIP Publishing LLC.

Fabrication of uniform Ge-nanocrystals embedded in amorphous SiO_2 films using Ge-ion implantation and neutron irradiation methods

Q. Chen,[1] T. Lu,[1,a)] M. Xu,[2,b)] C. Meng,[3] Y. Hu,[1] K. Sun,[4] and I. Shlimak[5]
[1]*Department of Physics and Key Laboratory for Radiation Physics and Technology of Ministry of Education, Sichuan University, Chengdu 610064, People's Republic of China*
[2]*Institute of Solid State Physics, Sichuan Normal University, Chengdu 610068, People's Republic of China and International Center for Material Physics, Chinese Academy of Sciences, Shenyang 110016, People's Republic of China*
[3]*Key Lab for Shock Wave and Detonation Physics Research, Institute of Fluid Physics, Chinese Academy of Engineering Physics, Mianyang 621900, People's Republic of China*
[4]*Department of Materials Science and Engineering and Electron Microbeam Analysis Laboratory, The University of Michigan, Ann Arbor, Michigan 48109-2143, USA*
[5]*Department of Physics, Minerva Center and Jack and Pearl Resnick Institute of Advanced Technology, Bar-Ilan University, Ramat-Gan 52900, Israel*

(Received 9 October 2010; accepted 21 January 2011; published online 14 February 2011)

Uniform Ge-nanocrystals (Ge-ncs) embedded in amorphous SiO_2 film were formed by using $^{74}Ge^+$ ion implantation and neutron transmutation doping (NTD) method. Both experimental and theoretical results indicate that the existence of As dopants transmuted from ^{74}Ge by NTD tunes the already stabilized (crystallized) system back to a metastable state and then activates the mass transfer processes during the transition form this metastable state back to the stable (crystallized) state, and hence the nanocrystal size uniformity and higher volume density of Ge-ncs. This method has the potential to open a route in the three-dimensional nanofabrication. © *2011 American Institute of Physics*. [doi:10.1063/1.3553770]

Research on quantum dots (QDs) or nanocrystals with a discrete energy spectrum and size-dependent physical properties is motivated by potential applications.[1–5] Future studies on smaller technological devices at the nanometer scale will emphasize techniques for creating nanocrystals with better size uniformity.[6] Photoluminescence (PL) results show that the best PL response from Ge-nanocrystals (Ge-ncs) in amorphous silicon oxide films was obtained with samples that exhibit uniform nanocrystal size.[7] Uniform shape and ordered size distribution nanocrystals are necessary in quantum-dot lasers.

In extensively utilized self-assembly methods, the QDs have a random spatial distribution, and it is difficult to precisely control dot size.[8] Several attempts have been made recently to improve the uniformity of QD distribution.[6,9–14] However, thus far only two-dimensional periodic array uniform QDs have been obtained. Achieving uniform QDs under the 3D confinement conditions remains one of the most daunting challenges (in quantum-dot formation, etc). Neutron transmutation doping (NTD) is a technique which utilizes the nuclear reaction of thermal neutrons with the isotopes in a semiconductor material,[15–17] and it has been reported that impurities are distributed homogeneously in a material[18–22] by using NTD. In this letter, we report that Ge-ncs are doped by As atoms by using NTD.

The preparation of uniform Ge-ncs is as follows. The isotope nanocrystalline ^{74}Ge samples were prepared by isotopic ^{74}Ge-ion implantation, followed by thermal annealing. Ion implantation was performed in a LC-4 high-energy ion implanter in a 10^{-5} Torr vacuum atmosphere. Gas GeH_4 was ionized into Ge^+ and Ge^{2+} by arc discharging. Isotope $^{74}Ge^+$ ions accelerated to 150 keV were selected by magnetism analysis equipment (the mass resolution of magnet $m/\Delta m = 120$), and implanted into a 640 nm thick amorphous SiO_2 film, which was thermally grown on a p-type [100] Si matrix. The implanted dose of $^{74}Ge^+$ ions was 1×10^{17} cm^{-2}. After implantation, samples were annealed at 800 °C for 0.5 h in a forming gas (10% H_2 and 90% Ar) atmosphere (labeled as undoped Ge-ncs). Neutron irradiation was performed in a nuclear reactor by laying the samples in the nuclear reactor, with integral thermal neutron fluence of 1×10^{20} cm^{-2}. Donor impurity ^{75}As is transmuted from ^{74}Ge by NTD,

$$^{74}\mathrm{Ge}(\mathrm{n},\gamma) \rightarrow {}^{75}\mathrm{Ge}^{T(1/2)\_82.8\ \mathrm{min}} \rightarrow {}^{75}\mathrm{As}(\beta^-\mathrm{decay}). \quad (1)$$

Second annealing is at 800 °C to eliminate any irradiation-induced defects and to recrystallize the Ge-ncs (labeled as doped Ge-ncs).

Cross-section and high-resolution transmission electron microscope (TEM) images were obtained with JEOL 2010 FEG transmission electron microscopy. X-ray photoelectron spectroscopy (XPS) spectra were measured by Ultra-DLD XPS, with a mono-Al source operated at a vacuum of 3×10^{-9} Torr. The presence of As atoms was proved by the XPS spectrum. Figure 1(e) shows the low-energy regions of XPS spectra of the undoped and doped Ge-nc samples. The broad bands from 23 to 33 eV and 40 to 50 eV correspond to Ge, SiO_2, and As impurities. The positions of the peaks are 25.3 eV for O 2s from SiO_2, 29.1 eV for Ge 3d from Ge, 33.2 eV for Ge 3d from GeO_2, 40.7 eV for As 3d from As, 44.8 for As 3d from As_2O_3, and 46.0 eV for As 3d from As_2O_5.[23] Figure 1(d) shows the size distributions of the undoped and doped samples. An area containing approximately 40 dots was analyzed. The mean sizes are 10.2 nm for the undoped sample and 11.5 nm for the doped sample. The

a)Electronic mail: lutiecheng@scu.edu.cn.
b)Electronic mail: hsuming_2001@yahoo.com.cn.

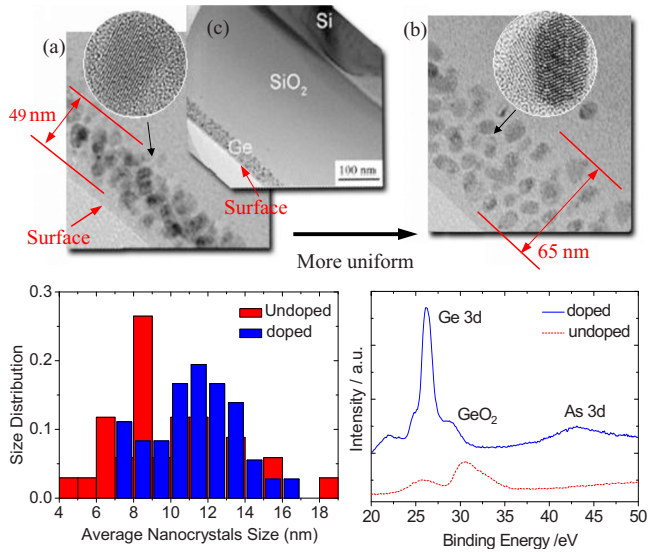

FIG. 1. (Color online) Cross-section TEM images of [(a) and (c)] undoped Ge-ncs and (b) doped Ge-ncs. (d) Size distributions of the undoped and As-doped Ge-ncs. (e) XPS analysis of undoped and As-doped Ge-ncs.

average size increases with introducing impurities in the sample. The size distribution of doped sample (7–17 nm) is narrower than the undoped case (4–19 nm). The insets in Figs. 1(a) and 1(b) show the cross-section TEM images of the undoped and doped Ge-ncs. We can clearly see that the size and distribution of the doped sample are more uniform than those of the undoped one, and that the volume density of nanocrystals increased by 13.11%.

To understand the formation mechanism of uniform Ge-ncs, we have performed interaction studies between As atoms and Ge nanocrystal using the *ab initio* density functional method performed with the DEMOL[3] code,[24] in which the local-density approximation in the scheme of Perdew–Wang 1992 the Perdew-Wang-correlation (Ref. 25) and the generalized-gradient approximation in the scheme of Perdew–Burke–Ernzerhof[26] are used. According to the formation energy calculation (no shown here), an As atom favors an interstitial site in Ge nanocrystal. Figure 2(a) shows the {220} face spatial distribution related to the highest occupied molecular orbital (HOMO) of Ge-ncs with an As atom doping in an interstitial site, where it is the most stable site of As atom in Ge nanocrystal. For comparison, the spatial distribution of the O case is shown in Fig. 2(b). The HOMO is especially important in determining the chemical reactivity of a system. We can see that the HOMO states progressively localize on the impurities. Red and blue regions indicate electron accumulation and loss, respectively. For the O-doping case, since the charges mainly accumulate in the middle of the bond and are shared with each other, covalent contact is predominant. For the As doping case, electron accumulation and loss around the As atom are obvious, as ionic contact is predominant between the As and Ge atoms in nanocrystal.

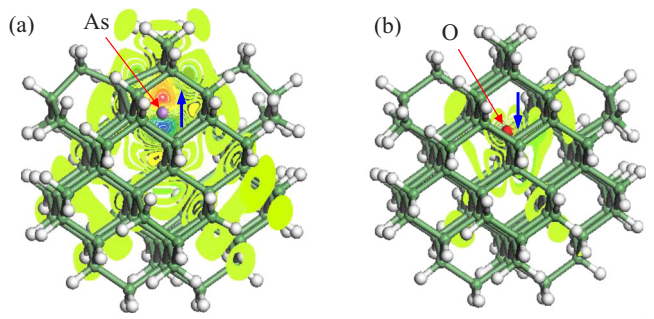

FIG. 2. (Color online) Spatial distribution related to the HOMO of (a) As- and (b) O-doped Ge-ncs.

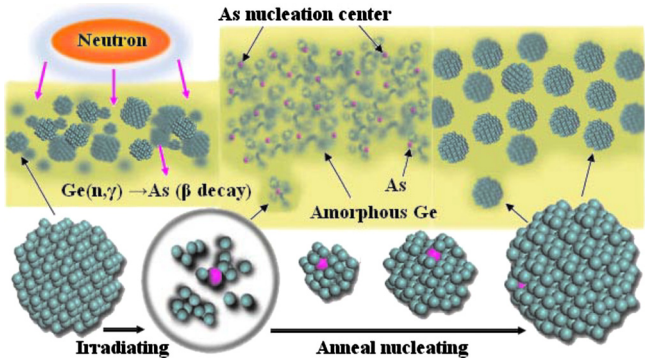

FIG. 3. (Color online) Scheme of system considered.

Significant changes were found in the Ge–Ge bond length after introducing an As atom into the nanocrystal. We can see that the distortion of nanocrystal is obvious after As doping. The formation energy of As-doped nanocrystals is smaller than the O-doped nanocrystals. For example, the average Ge–Ge bond length ($\bar{L}$) increases to 2.68 Å, 4.69% higher than the undoped case (2.56 Å). However, the average value for O-doping is 2.55 Å, indicating that doping with As produces a greater distortion. The deflection of impurity atoms from the center of local symmetry of doped nanocrystal interstitial sites (labeled as Ω center) was also found. The distance increases from 2.89 Å (between the Ω center and the Ge atom in the center of nanocrystal) to 3.13 Å (between the As atom in interstitial site and the Ge atom in the center site of nanocrystal) after the As doping and geometry optimization. Otherwise, for the O-doping in the same interstitial site, the distance between the O atom and the center of the nanocrystal is 2.04 Å after geometry optimization. A large repulsion force between the As atoms and Ge-ncs is indicated.

A possible formation mechanism of the Ge nanolayer may be discussed as follows (see Fig. 3). Lu *et al.*[27] insisted that the Debye length is given by

$$l_D = \sqrt{\varepsilon_s k_B T/(q^2 N_d)}, \tag{2}$$

where ε_s is the permittivity of the substrate, k_B the Boltzmann constant, T the temperature, q the charge of one electron, and N_d the donor density in the substrate. When two Ge-ncs approach each other, the accompanying charge clouds overlap, leading to a repulsive force that prevents them from coalescing. Significant repulsion appears when the separation of two Ge-ncs reduces to a scale comparable to l_D. An energy barrier appears at a separation of approximately $0.02l_D$, below which van der Waals interaction dominates and drives two Ge-ncs into contact. A silicon substrate has $\varepsilon_s = 3.9\varepsilon_0$, where ε_0 is the permittivity of vacuum. Using $\varepsilon_0 = 8.85 \times 10^{-12}$ F/m, $q = 1.60 \times 10^{-19}$ C, $k_B = 1.38 \times 10^{-23}$ J/K, $T = 300$ K, and $N_d = 5 \times 10^{13}$ cm^{-3}, we have $l_D = 334.1$ nm. In Fig. 1(a), we cannot see the separation of Ge-ncs from the inset TEM image, and the distance between

the two Ge-ncs is about 10 nm, much smaller than the calculated Debye length. This leads us to infer that there may be some other mechanism of uniform nucleation.

Followed by the ^{74}Ge ion implantation, primary thermal annealing, neutron irradiation, and a subsequent reannealing, the nucleation mechanism of As-doped Ge-ncs is extraordinarily complex, including damage-enhanced diffusion and interfacial-energy effects. Nonetheless, the size distributions become more uniform after introducing As into Ge-ncs. The local high-temperature nucleates Ge ions into Ge-ncs after Ge-ion implantation. Annealing due to the minimum energy principle is then carried out, because the Gibbs free energy of a nanoparticle aggregated from ions is much lower than the energy sum of these ions. The dopant atoms are usually not in their lattice positions but displaced in interstitial positions or isolated points due to the recoil produced by the γ- and β-particles and the lower formation energy in Ge-nc interstitial sites. After irradiation, As separates from Ge-ncs and creates more nucleation sites. Due to the large repulsion force between As atoms and Ge-ncs, the As nucleation sites are 3D positional uniform. In addition to producing As donors, the neutron irradiation shakes and breaks the Ge-ncs, which becomes amorphous state, introducing more defects. The irradiated samples were subjected to the second annealing to eliminate any irradiation-induced defects and to recrystallize the Ge-ncs around the As nucleation center. There are counterbalances between nucleation and spinodal decomposition during nanocrystal formation. During the process of nucleation, each Ge nanocrystal in samples deforms laterally to match the amorphous SiO_2 substrate. The deformation induces a tensile stress region in the substrate below. According to the calculation, the distortion of Ge-ncs is larger after As doping, as shown in Fig. 2(a). Doping with As leads to greater charge cloud density and distortion. The strain fields from misfit dislocation make the sizes and spacing of sample more uniform.

The net concentration of NTD-introduced impurities (N_{NTD}) is

$$N_{\mathrm{NTD}} = N_0 k_i \delta_i \varphi t, \tag{3}$$

where N_0 is the concentration of Ge atoms in the lattice (cm^{-3}), k_i is the abundance of ^{74}Ge isotopes, φ is the intensity of the thermal neutron flux (thermal neutrons/cm^2 s), t is the exposure time (s), and δ_i is the thermal neutron capture cross-section (for ^{74}Ge, $\delta_i = 0.5 \times 10^{-24}$ cm^2). From this equation, the dimensionless ratio $N = N_{\mathrm{As}}/N_{\mathrm{Ge}}$ is determined to be 5×10^{-5} in doped Ge-ncs. Mean sizes are 10.2 nm for the undoped sample and 11.5 nm for the doped sample. Then one As atom can attract about 1×10^4 Ge atoms during annealing and form a nanocrystal. The SiO_2–Ge system became metastable and "soft" after irradiation. Until the matter has recrystallized, the Ge atoms channeled (diffused) between the existing nanoparticles, improving size uniformity.

In summary, As-doped Ge-ncs have been embedded in amorphous SiO_2 film by using $^{74}Ge^+$ ion implantation and the NTD method. Both experiments and theories show that the As dopants have a great influence on the uniformity of Ge-ncs. By turning the already stabilized (crystallized) system back to a metastable state and then activating the mass transfer processes during the transition from this metastable state back to the stable (crystallized) state, nanocrystal size uniformity was improved. We report a method that creates semiconductor Ge quantum dots with high uniformity and high density, showing promising applications in three-dimensional nanofabrication.

This project was supported by the NASF of NSFC-CAEP of China (Grant No. 10376020), the Program for New Century Excellent Talents in University (Grant No. NCET-04-0874), and Sichuan Youth Science & Technology Foundation, China (Grant No. 08ZQ026-025). We thank Dr. Levchenko and Professor Ostrikov at CSIRO Material Science and Engineering of Australia for their helpful discussion.

[1] S. Ghosh, W. H. Wang, F. M. Mendoza, R. C. Myers, X. Li, N. Samarth, A. C. Gossard, and D. D. Awschalom, Nature Mater. **5**, 261 (2006).
[2] J. Witzens and A. Scherer, Nature Mater. **4**, 512 (2005).
[3] J. C. Johnson, H. J. Choi, K. P. Knutsen, R. D. Schaller, P. Yang, and R. J. Saykally, Nature Mater. **1**, 106 (2002).
[4] M. T. Hill, Nat. Nanotechnol. **4**, 706 (2009).
[5] F. J. Garcia-Vidal and E. Moreno, Nature (London) **461**, 604 (2009).
[6] J. D. Budai, C. W. White, S. P. Withrow, M. F. Chisholm, J. Zhu, and R. A. Zuhr, Nature (London) **390**, 384 (1997).
[7] W. K. Choi, Y. W. Ho, S. P. Ng, and V. Ng, J. Appl. Phys. **89**, 2168 (2001).
[8] K. Alchalabi, D. Zimin, G. Kostorz, and H. Zogg, Phys. Rev. Lett. **90**, 026104 (2003).
[9] J. Tersoff, C. Teichert, and M. G. Lagally, Phys. Rev. Lett. **76**, 1675 (1996).
[10] S. Y. Shiryaev, F. Jensen, J. L. Hansen, J. W. Petersen, and A. N. Larsen, Phys. Rev. Lett. **78**, 503 (1997).
[11] M. A. Lutz, R. M. Feenstra, F. K. LeGoues, P. M. Mooney, and J. O. Chu, Appl. Phys. Lett. **66**, 724 (1995).
[12] X. Qian, J. Li, D. Wasserman, and W. D. Goodhue, Appl. Phys. Lett. **93**, 231907 (2008).
[13] T. Ujihara, Y. Yoshida, W. S. Lee, and Y. Takeda, Appl. Phys. Lett. **89**, 083110 (2006).
[14] P. A. Crozier, C. Ritter, J. Tolle, and J. Kouvetakis, Appl. Phys. Lett. **84**, 3441 (2004).
[15] S. Dun, T. Lu, Y. Hu, Q. Hu, C. You, and N. Huang, Mater. Lett. **62**, 3617 (2008).
[16] Y. Hu, T. Lu, S. Dun, Q. Hu, N. Huang, S. Zhang, B. Tang, J. Dai, L. Resnick, I. Shlimak, S. Zhu, Q. Wei, and L. Wang, Solid State Commun. **141**, 514 (2007).
[17] Y. Hu, T. Lu, S. Dun, Q. Hu, C. You, Q. Chen, N. Huang, L. Resnick, I. Shlimak, K. Sun, and W. Xu, Scr. Mater. **61**, 970 (2009).
[18] M. Satoh, K. Kuriyama, and T. Kawakubo, J. Appl. Phys. **67**, 3542 (1990).
[19] J. Grun, C. K. Manka, C. A. Hoffman, J. R. Meyer, O. J. Glembocki, R. Kaplan, S. B. Qadri, E. F. Skelton, D. Donnelly, and B. Covington, Phys. Rev. Lett. **78**, 1584 (1997).
[20] M. Satoh, K. Kuriyama, M. Yahagi, K. Iwamura, C. Kim, T. Kawakubo, K. Yoneda, and I. Kimura, Appl. Phys. Lett. **50**, 580 (1987).
[21] K. Kuriyama, M. Yahagi, K. Iwamura, Y. Kim, and C. Kim, J. Appl. Phys. **54**, 673 (1983).
[22] K. Kuriyama, K. Sakai, and M. Okada, Phys. Rev. B **53**, 987 (1996).
[23] J. F. Moulder, W. F. Stickle, P. E. Sobol, and K. D. Bomben, *Handbook of X-Ray Photoelectron 165 Spectroscopy* (Perkin-Elmer Corp., USA, 1992).
[24] S. Nigam, C. Majumder, and S. K. Kulshreshtha, J. Chem. Phys. **121**, 7756 (2004).
[25] J. P. Perdew and Y. Wang, Phys. Rev. B **45**, 13244 (1992).
[26] J. P. Perdew, K. Burke, and M. Ernzerhof, Phys. Rev. Lett. **77**, 3865 (1996).
[27] W. Lu and D. Salac, Phys. Rev. B **74**, 073304 (2006).